applied sciences

MDPI

Review

Ultrafast and Wideband Microwave Photonic Frequency-Hopping Systems: A Review

Qidi Liu and Mable P. Fok *

Lightwave and Microwave Photonics Laboratory, College of Engineering, The University of Georgia, Athens, GA 30602, USA; qidi.liu@uga.edu

* Correspondence: mfok@uga.edu; Tel.: +1-706-542-2233

Received: 29 November 2019; Accepted: 26 December 2019; Published: 10 January 2020

Abstract: The increasing demands to enhance information security in data transmission, providing countermeasures against jamming in military applications, as well as boosting data capacity in mobile and satellite communication, have led to a critical need for high-speed frequency-hopping systems. Conventional electronics-based frequency-hopping systems suffer from low data rate, low hopping speed, and narrow hopping-frequency bandwidth. Unfortunately, those are important aspects to facilitate frequency-hopping in emerging microwave systems. The recent advancement of microwave photonics—the use of light to process microwave signals—provides promising solutions to tackle the challenges faced by electronic frequency-hopping systems. In this paper, the challenges of achieving real-time frequency-hopping systems are examined. The operation principles and results of various microwave photonics-enabled frequency-hopping systems are comprehensively discussed, which have wide hopping-frequency bandwidth and frequency-hopping speed from nanoseconds to tens of picoseconds. Lastly, a bio-inspired jamming-avoidance system that could potentially be used for adaptive frequency-hopping is also introduced.

Keywords: microwave photonics; frequency-hopping; photonic signal processing

1. Introduction

Frequency-hopping systems, which change the information carrier frequency between a series of frequencies determined by a unique hopping code sequence (Figure 1), has always attracted great interest in radar and satellite systems, wireless radio frequency (RF) communications, as well as emerging dynamic communication systems (i.e., 5G/6G) [1]. The history of frequency-hopping dates to 1941, when it was patented by a Hollywood actress Hedy Lamarr and pianist George Antheil. The technology was not taken seriously in electronic countermeasures worldwide until the 1980s. With the merit of frequency-hopping systems, such as mitigating the effects of inter-symbol interference and jamming, it significantly increases the communication capacity of emerging RF wireless systems—making it an essential tool to fulfil the high RF spectral resource demand in the commercial, defense, and civilian federal marketplaces [2–4]. Furthermore, the fast frequency-hopping capability greatly increases the security of wireless services—the lack of amplitude variations and fast-changing in carrier frequency makes it challenging for Eve to interpret the information. Moreover, signal interference resulting from multi-path effects could be largely reduced by fast-changing frequency carriers. Frequency-hopping systems have been widely implemented, e.g., in Bluetooth [5], Advanced Extremely High-Frequency (AEHF) communications satellites [6], and the Military Strategic and Tactical Relay (MILSTAR) communication satellites [7]. Although frequency-hopping systems have been proved successfully in various RF systems, the hopping speed is limited to milliseconds, and the hopping-frequency bandwidth is less than several GHz, which hinders its implementation in emerging RF wireless communications and sophisticated electronic warfare systems. Due to the

inherent electronic bottleneck and available frequency bandwidth of electronic devices, it is very challenging for electronics-based frequency-hopping systems to achieve hopping-frequency bandwidth over several GHz in close to real-time hopping speed.

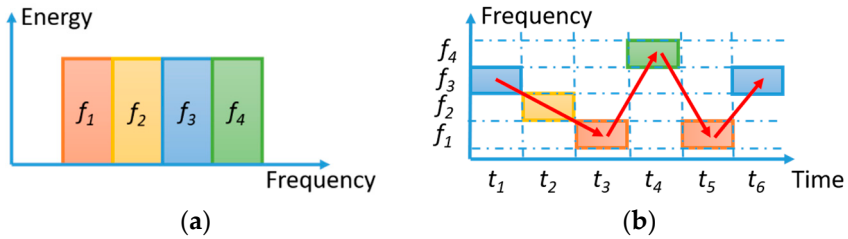

Figure 1. Principle of frequency-hopping communication systems. (**a**) Frequency channel assignment for a single user; (**b**) Time-varying spectral usage of the allocated frequency for a particular user.

Microwave photonics (MWP), which bridges RF signal and photonic signal processing, is capable of overcoming bottlenecks in electronics due to its large bandwidth, instantaneous response, as well as flexibility and reconfigurability [8]. Various RF signal processing tasks have been successfully demonstrated using photonic technologies [9–19], such as MWP analog-to-digital converters, MWP filters, MWP arbitrary waveform generators, MWP image rejection mixer, and MWP frequency measurement, to name a few. Although microwave photonic approaches are capable of generating various types of RF signals [20], it is not trivial to use them for generating frequency-hopping signals due to the limited frequency tunability and hopping speed in the existing signal generating approaches, as well as the time required to stabilize at the desired frequency.

In this review paper, we will first introduce the operation principle and configuration of several frequency-hopping systems based on microwave photonics. Several recent breakthroughs in microwave photonic frequency-hopping signal-generation schemes that enable ultrafast and wideband operation are compared. In Section 3, a bio-inspired photonic circuit mimicking the jamming-avoidance system in a gene of electric fish is presented, which has great potential in facilitating an adaptive frequency-hopping system. Finally, the paper is concluded by a discussion of the existing frequency-hopping techniques and their potential in dynamic and wideband RF signal processing.

2. Microwave Photonic Frequency-Hopping Systems

Microwave photonic frequency-hopping systems have wider hopping bandwidth and roughly 10^3–10^6 times faster hopping speed when compared with conventional electronic approaches. Figure 2 shows an illustration of a microwave photonic frequency-hopping system that consists of a pre-encoded input data module shown in Figure 2a, and a frequency-hopping carrier generation module for generating the uplink carrier shown in Figure 2b,c. The pre-encoded input data is used to modulate the RF carrier and then transmitted through a high-frequency antenna as a frequency-hopping signal. There are mainly two types of MWP frequency-hopping carrier generation schemes, including (i) MWP frequency synthesizer with ultrafast frequency switching ability, such as the use of nonlinear period-one dynamics of injected semiconductor laser to directly generate different frequency at different time [21,22]; (ii) MWP switch for fast switching of pre-generated frequencies, such as the use of ultrafast microwave photonic RF filter to switch out different frequency carriers.

There are two major challenges in MWP frequency synthesizer approach: First, it is the need to establish a stable desired frequency in a short period to enable fast frequency switching; second, the precise control of the hopping code sequence properties due to the required tight relationship between the synthesized frequency and the applied hopping code sequence. In MWP RF switch approaches, the two major challenges are: (i) achieving fast switching time within a cycle of the carrier, and (ii) the ability to completely switch off the unwanted frequencies. For both approaches, it is even more challenging to achieve a multi-level frequency-hopping system with picoseconds

hopping speed and instantaneous reconfiguring capabilities. Table 1 shows a list of examples of the state-of-the-art frequency-hopping signal-generation schemes based on various RF electronics and microwave photonic approaches. In this section, we discuss and compare the principles, hopping speed, flexibility in the hopping frequency, and hopping-frequency bandwidth of various microwave photonic frequency-hopping signal-generation schemes.

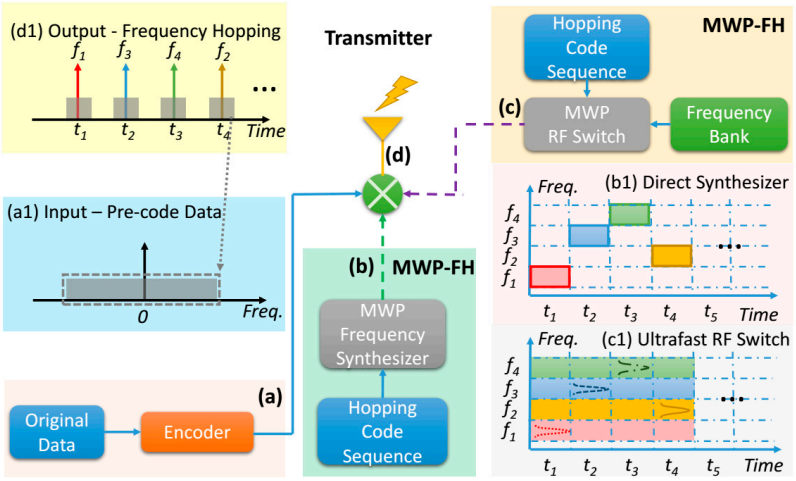

Figure 2. Schematic of microwave photonic frequency-hopping transmission systems. (**a**) Input—encoded data at baseband; (**b**) Ultrafast MWP-based frequency synthesizer controlled by an applied hopping pattern. (**c**) Frequency-hopping carrier generation using MWP RF switch (**d**) Output—frequency-hopping signal.

Table 1. Comparison of the State-of-the-Art Frequency-Hopping Signal-Generation Schemes.

Reference	Techniques	Speed	Potential for Multi-level	Methods	Tuning Mechanism
[23]	Four wave mixing	50 ps	No	switch	Polarization tuning
[24]	SBS filter	100 ps	Yes	switch	SBS tuning
[25]	EO-based comb filter	100 ps	Yes	switch	EO Pockels effect
[26]	Notch filter	190 ps	No	switch	EO Pockels effect
[27]	Lyot filter	200 ps	Yes	switch	Nonlinear polarization rotation
[28]	DD-MZM bias control	1 ns	No	switch	EO Pockels effect
[29]	Optical injection	10 ns	Yes	synthesizer	Nonlinear dynamics
[30]	Delay line-based comb filter	40 ns	Yes	switch	Optical delay line
[31]	PM-PSFBG OEO	100 ns	Yes	synthesizer	Polarization tuning
[32]	Microring resonator	500 us	Yes	synthesizer	Thermal tuning
[33]	RF-MEMS	300 us	Yes	switch	MEMS capacitor
[34]	Integrated spectrum shaper	7 ms	Yes	switch	Thermal tuning

2.1. Microwave Photonic Opto-Electronic Oscillator Enabled Frequency-Hopping System

Opto-electronic oscillator (OEO) has attracted great interest for decades [35–37] to replace the conventional RF signal generator for applications that have precise timing requirement due to the OEO's high stability and low phase noise performance over a wide frequency bandwidth. OEO usually consists of a laser source, an electro-optic modulator, a section of optical fiber, a photodetector, an electrical amplifier, a microwave bandpass filter, and an electrical power coupler, such that the RF signal is repeatedly selected by an electrical bandpass filter and amplified to ensure gain is larger than the loss in the OEO cavity to achieve a high-Q factor. Once the accumulated gain and phase of the oscillation condition are satisfied, high quality microwave signal is resultant, where the oscillating frequency is governed by the center frequency of the microwave bandpass filter. To generate

frequency-hopping signal using OEO, the center frequency of the microwave bandpass filter must be changed rapidly according to the applied hopping code sequence. Unfortunately, microwave bandpass filters have narrow frequency tuning range and slow tuning speed due to the inherent limitation in tuning mechanism, making it not suitable for high-speed and large dynamic range frequency-hopping generation [38,39]. To solve this problem, microwave photonic filter is used in place of the microwave bandpass filter that is incorporated in the OEO.

Figure 3a shows the use of a polarization-maintaining phase-shifted fiber Bragg grating (PM-PSFBG)-based OEO for the generation of wideband frequency-hopping signal [31]. The polarization modulator (PolM), optical circulator, PM-PSFBG, and photodetector form an MWP filter. When the PM-PSFBG is used with a PolM, the MWP filter exhibits a polarization-dependent RF response with narrow 3-dB bandwidth, as illustrated on the right of Figure 3b. It is important to note that there are two notches in the PM-PSFBG reflection spectrum for each principal polarization axis of the PM-PSFBG to achieve phase to intensity conversion during photodetection. Therefore, two different frequency responses, each with two transmission peaks are observed through a vector network analyzer (VNA), as shown in Figure 3b. To achieve frequency-hopping signal generation, polarization of a continuous wave light wave is aligned at 45° with respect to the principal axis of the PolM for polarization modulation. The modulated light is then sent to PM-PSFBG via an optical coupler (OC) such that the light will go through both the principle polarization axes of the PM-PSFBG. The reflected signal is detected by a photodetector and an ultra-narrow (~40 MHz) passbands are observed at the microwave photonic filter. The resultant hopping frequency is determined by the power distribution between the two PM-PSFBG axes (i.e., governed by the control signal, i.e., the hopping code sequence applied to the PolM) and the frequency spacing between the laser wavelength and notches at the MWP filter.

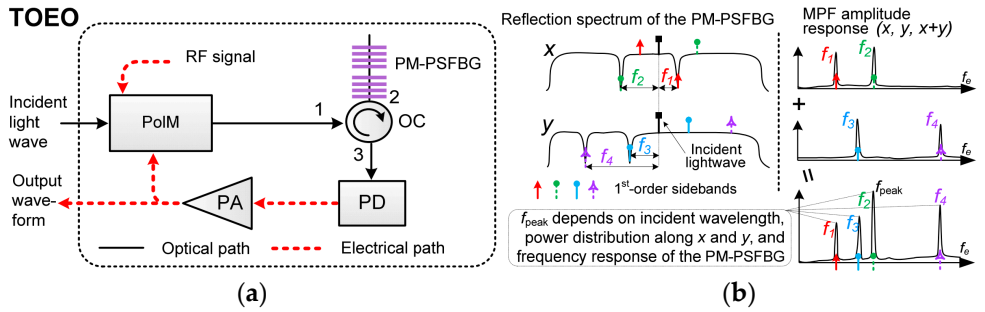

Figure 3. (**a**) Schematic diagram of an OEO-based frequency-hopping signal-generation scheme. PoIM: polarization modulator; OC: optical coupler; PD: photodetector; PA: electrical power amplifier. (**b**) Operation principle of the OEO (with the courtesy of Dr J. Yao).

Therefore, by changing the laser wavelength, modifying the DC voltage applied to the PolM, and adjusting the light polarization launching to the PM-PSFBG, frequency-hopping RF signal can be generated. Figure 4a,b show two resultant frequency-hopping signals that successfully hop between 17.1 GHz and 15.75 GHz as well as 9.58 GHz and 8.65 GHz, respectively, with 100 ns hopping speed. Although frequency-hopping signal can be generated using MWP filter-based OEO scheme, there are still room for improvements in the following aspects: (1) reduction of the long establishment time of oscillating mode to increase frequency-hopping speed; (2) improvement of signal phase noise that was currently deteriorated due to uncorrelated phase relationship between adjacent oscillation modes; (3) achieving multi-level frequency-hopping signal generation that is currently hindered by mode competition in the OEO.

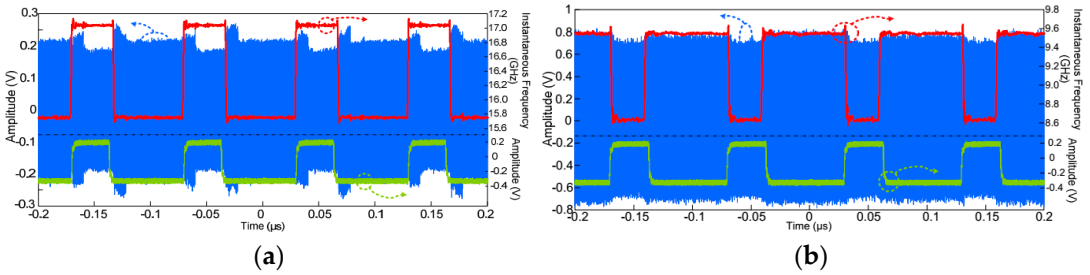

Figure 4. Measured hopping code sequence (green), waveform of the generated frequency-hopping microwave signal (blue), and the calculated instantaneous frequency of the frequency-hopping signal (red). (**a**) Frequency-hopping between 17.1 GHz and 15.75 GHz; (**b**) Frequency-hopping between 9.58 GHz and 8.65 GHz (with the courtesy of Dr J. Yao).

2.2. Frequency-Hopping through Period-One Nonlinear Dynamcis in Semiconductor Lasers

When a slave semiconductor laser experiences optical pumping from a master laser, various nonlinear dynamics can be excited, such as chaotic dynamics, injection locking dynamics, and periodic oscillations [21,22,40,41]. Depending on the detuning frequency, injection power ratio, as well as the controlling of polarization relationship between the slave and master lasers, different nonlinear dynamics and characteristics could be induced. Among all the nonlinear dynamics in semiconductor lasers, period-one (P1) dynamics is a good candidate to achieve frequency-hopping due to its unique spectral phenomenon as well as fast hopping speed of up to nanoseconds range.

The schematic diagram of period-one dynamics-based frequency-hopping system [29] is shown in Figure 5a. A master laser that is emitting continuous wave at f_m is attenuated and then intensity modulated by a hopping code sequence $S(t)$. The modulated master laser light is launched to a free running slave laser at f_s via an optical circulator. The lasing frequency difference between the master and slave lasers is f_s. Through injection locking, the master laser pulls the slave laser oscillating frequency towards the master laser frequency f_m by locking its phase, forcing the slave laser to lase at f_m. At the same time, the gain region of the slave laser is red-shifted (i.e., shifting f_s to f_s') due to the refractive index change inside the cavity resulted from an increase in carrier density through master laser light injection. Therefore, the two effects compete—injection-induced gain region shifting to red while phase locking from master laser shift the lasing to blue, leading to period-one nonlinear dynamics, i.e., the slave laser lases at both f_m and f_s'. As illustrated in Figure 5b, a RF signal with frequency f_o results after photodetection, which is governed by the frequency difference between the two lasing frequencies of the slave laser ($f_o = f_m - f_s$'). The observed asymmetric double-sideband spectrum is due to Hopf bifurcation. The resultant lasing frequency f_s' due to refractive index change is determined by the strength of the injection light. Therefore, frequency of the resultant RF signal can be adjusted through the control of the injection light power.

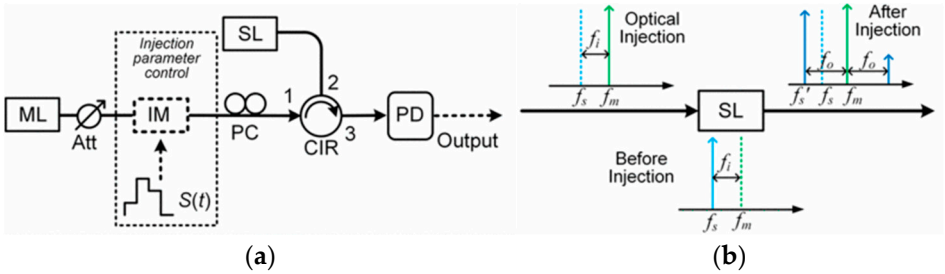

Figure 5. (**a**) Schematic diagram of the period-one (P1) nonlinear dynamic-based frequency-hopping signal-generation scheme. (**b**) Operation principle of P1 dynamics in an optically injected semiconductor laser. ML: master laser, Att: optical attenuator; IM: intensity modulator, S(t): hopping code sequence; PC: polarization controller, CIR: optical circulator; SL: slave laser, PD: photodetector (with the courtesy of Dr S. Pan).

Figure 6a–c show the temporal measurement of the generated RF signal under different injection conditions, while the corresponding hopping code sequence $S(t)$ is shown in the insets. The injection strength is defined as ξ, which is proportional to the injected power. Therefore, for a fixed detuning frequency $f_i = f_s - f_m$, the generated RF signal frequency f_o would increase linearly with the injection amplitude. Therefore, by controlling the optical injection power using a hopping code sequence, frequency-hopping signal can be generated. Figure 6d–f shows the measured instantaneous frequency of the generated RF signal. By setting the hopping code sequence to a two-level square wave, frequency-hopping signal with frequencies at 13.1 and 17.6 GHz is resultant. Thanks to the fast P1 dynamic response, ~10 ns hopping speed is demonstrated. P1 dynamic-based frequency-hopping signal-generation scheme can generate multi-level frequency-hopping signal. With a four-level hopping code sequence, the resultant frequency-hopping signal can hop between four different frequencies, as shown in Figure 6e,f. Since the resultant frequency greatly depends on the injection light amplitude, it is important to reduce amplitude fluctuation in the injection light to prevent instability in the frequency-hopping signal frequency.

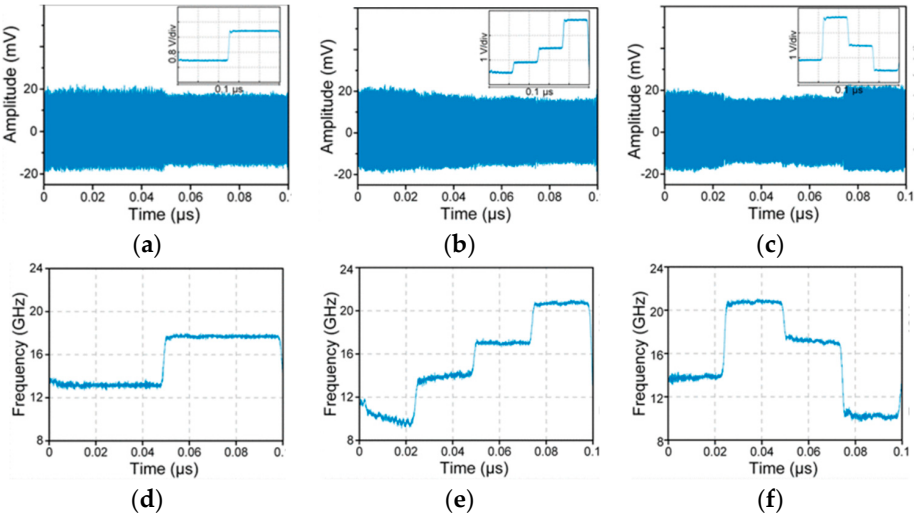

Figure 6. (**a**–**c**) Measured temporal waveforms of the frequency-hopping signal under different injection conditions. (Insets) Corresponding hopping code sequence S(t). (**d**–**f**) Recovered instantaneous frequency corresponding to (**a**–**c**), respectively (with the courtesy of Dr S. Pan).

2.3. Bias Control in Dual-Drive Mach–Zehnder Modulater for Frequency-Hopping Signal Generation

To achieve a faster frequency-hopping speed, Pockels effect in a dual-drive Mach–Zehnder modulator (DD-MZM) is used [28], as illustrated in Figure 7a. In this approach, a reference microwave signal f_s with amplitude V_0 is injected into one arm of the DD-MZM, while a hopping code sequence $S(t)$ is applied to the other arm of the DD-MZM. The DC ports of the two arms are driven by a DC power supply to introduce phase difference. When a hopping code sequence $S(t)$ with an amplitude of V_s is applied to DD-MZM, the transmission function of the frequency-hopping system can be expressed as,

$$T = \frac{1}{2} + \cos\left[\frac{\pi(V_0 \cos(2\pi f_s t) - V_s S(t) - V_{DC})}{V_\pi}\right] \quad (1)$$

where V_π is the half wave voltage of the DD-MZM and V_{DC} is the DC bias difference between the two arms. As shown in Figure 7b, if V_{DC} is at the quadrature transmission point, the output RF signal is at the original reference signal frequency f_s due to the linear region in the transmission curve; while biasing at the minimum transmission point will lead to a doubling in output RF signal frequency (i.e., $2f_s$) due to the folding in the transmission curve. Thus, by setting the static DC bias at minimum transmission point and dynamically apply $S(t)$ to shift the bias to quadrature point, a frequency-hopping signal is resulted and can be expressed as,

$$i(t) = \begin{cases} \frac{1}{2}RE_0^2 - \frac{1}{2}RE_0^2 J_0(m) + RE_0^2 J_2(m)\cos(4\pi f_s t), & S(t) = 1 \\ \frac{1}{2}RE_0^2 + RE_0^2 J_1(m)\cos(2\pi f_s t), & S(t) = 0 \end{cases} \quad (2)$$

where R is responsivity of the PD and $m = \pi V_0/V_\pi$ is the modulation index. As shown in Figure 7c, the temporal waveform of the frequency-hopping signal indicates that the frequency is hopping between 12 GHz and 24 GHz when a 64-bit 1 Gbps pseudorandom binary sequence (PRBS) hopping code sequence is used. The hopping speed is measured to be 1 ns in this experiment. Since the DD-MZM has a higher modulation efficiency at the quadrature transmission point than that at the minimum transmission point, the generated frequency-hopping signal at f_s will always be stronger than the signal at $2f_s$, as shown in Figure 7c,d. Furthermore, the frequencies in the frequency-hopping signal will always have a fixed relationship of f_s and $2f_s$.

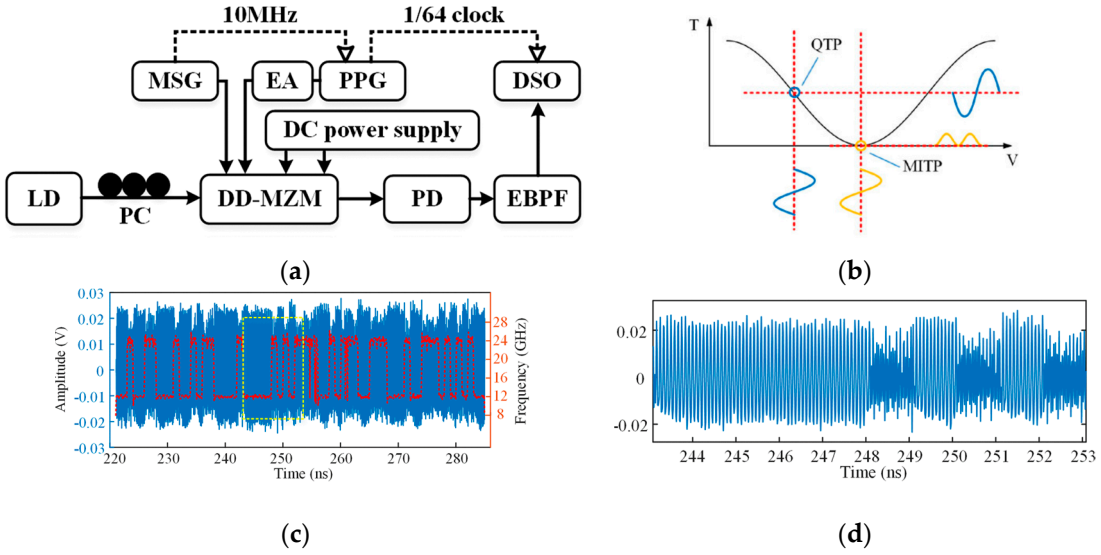

Figure 7. (**a**) Experimental setup of frequency-hopping signal generation by switching the bias point of an optical dual-drive Mach–Zehnder modulator: LD, laser diode; PC, polarization controller; DD-MZM, dual-drive Mach–Zehnder modulator; MSG, microwave signal generator; PPG, pulse pattern generator; EA, electrical amplifier; PD, photodetector; EBPF, electrical bandpass filter; DSO, digital sampling oscilloscope.; (**b**) Transmission characteristics of the DD-MZM at quadrature (QTP) and minimum (MITP) biasing points. (**c**) The measured frequency-hopping signal waveforms (blue solid line) and the calculated instantaneous frequencies (red dotted line). (**d**) A zoom-in view of the generated frequency-hopping RF signal in the yellow dotted line region in (**c**) (with the courtesy of Dr Y. Chen).

2.4. MWP RF Switch for Frequency-Hopping Signal Generation

Microwave switches, or RF switches are an essential tool in microwave systems for signal routing and signal modulation. RF switches usually have switching speed of hundreds of nanoseconds and operation bandwidth of several tens of GHz. To enable fast switching of RF signal for the generation of frequency-hopping signal, microwave photonic RF switches with switching time at tens of picosecond speed [42], which is way faster than any existing RF switch technologies, is a promising candidate. In this section, we will discuss two techniques to achieve high-speed RF switching—(1) Tunable microwave photonics filter, (2) Optical nonlinear wave mixing. The use of tunable microwave photonic filter with tens of gigahertz frequency tuning speed is an effective way to use microwave photonic technology for performing RF switching. MWP filters with single and multiple passbands have been intensively demonstrated using various techniques including the use of optical comb filter [25,43,44], stimulated Brillouin scattering (SBS) [24,45], and liquid crystal on silicon (LCoS) [46,47]. Various MWP filters could have slightly different pros and cons; for example, the use of SBS filter [24] could give a sharper MWP filter profile and results in a finer frequency resolution in the frequency-hopping

scheme. The use of an electrical delay line in a MWP filter [25] could limit the operation bandwidth of the frequency-hopping signal. However, most of the techniques have a fixed passband frequency or the tuning mechanism are based on manual control of tunable optical delay line, thermal tuning, or mechanical laser array tuning, which are too slow to achieve fast switching. To perform RF switching, only the techniques that are capable of fast tuning of the passband/bandstop frequency at GHz speed can be used. In this section, we will discuss several techniques for achieving high-speed RF signal switching for the generation of frequency-hopping signals.

2.4.1. Pockels Effect Based Fast Tunable MWP Switch for Frequency-Hopping Signal Generation

Pockels effect in $LiNbO_3$ modulators is well known for its fast response time in the order of tens of picosecond. By incorporating a $LiNbO_3$ phase modulator in a loop mirror filter, an ultrafast RF switch can be achieved, as shown in Figure 8a [26,48]. First, a single sideband modulated optical signal is generated at the dual-drive Mach–Zehnder modulator (DD-MZM), which is then launched into a phase modulator incorporated loop mirror filter (PM-LMF) for optical spectral filtering. If the RF spectral component in the single sideband optical signal is being blocked by the PM-LMF, the RF signal cannot be reconstructed at the photodetector and results in a notch in the frequency response at that particular frequency. The PM-LMF consists of a piece of polarization-maintaining fiber (PMF), a polarization controller (PC), a phase modulator (PM), and an OC. First, the input light is spilt into two branches at the OC, then the two light beams counter propagate in the LMF and interferer when they arrive at the OC again. Depending on the phase difference experienced by the two light beams, a periodic transmission function is resulted and can be expressed as,

$$T(\lambda) = \frac{1}{2}[1 - \cos(\varphi(\lambda))] \tag{3}$$

where $\varphi(\lambda)$ denotes the phase difference between the light travelling clockwise and anti-clockwise. Due to the total phase difference induced by both the PMF and a short tunable birefringence medium (e.g., PM), periodic optical comb response is resulted. When the transverse electric axis of the PM is aligned with the fast axis of the PMF, the corresponding comb spacing can be described as,

$$\Delta\lambda = \frac{\lambda^2}{B_{PMF}L_{PMF} + B_{PM}L_{PM}} \tag{4}$$

where B_{PMF}, L_{PMF}, B_{PM}, and L_{PM} are the birefringence and length of the PMF and PM, respectively. Birefringence of the PM is proportional to the electric field around the $LiNbO_3$ crystal waveguide. Therefore, the comb spacing can be shifted by controlling the applied DC voltage to the PM. Considering a small optical spectral region, a shift in the optical comb is observed, resulting in a shift in the transmission notch of the comb filter, as shown in Figure 8b. Since there is a direct corresponding between the transmission notch in the optical comb filter and the transmission notch in the RF filter, the RF transmission notch can also be tuned by controlling the DC voltage applied to the PM, as shown in Figure 8c.

To generate a frequency-hopping signal, two RF signals at f_1 and f_2 are modulated onto the optical carrier as a single sideband signal. A hopping code sequence with two voltage levels at V_1 and V_2 is used to control the birefringence of the PM, i.e., the RF transmission notch. When the RF notch is aligned with f_1, then only f_2 can be found at the output while f_1 is being blocked, or vice versa. Therefore, when the control signal is switched between V_1 and V_2, a frequency-hopping signal between f_1 and f_2 can be generated. As shown in Figure 8d, two-level frequency-hopping signal between 6 GHz and 12 GHz with 170 ps hopping speed is achieved by setting the applied voltage of bit "1" at 2.8 V and that of bit "0" at 0 V. Due to the fast response time of Pockels effect, hopping speed of tens of GHz can be achieved which is governed by the modulation bandwidth of PM. Although the hopping speed is fast, there is a requirement of the frequency separation between the hopping frequencies due to the periodicity and bandwidth of the MWP filter.

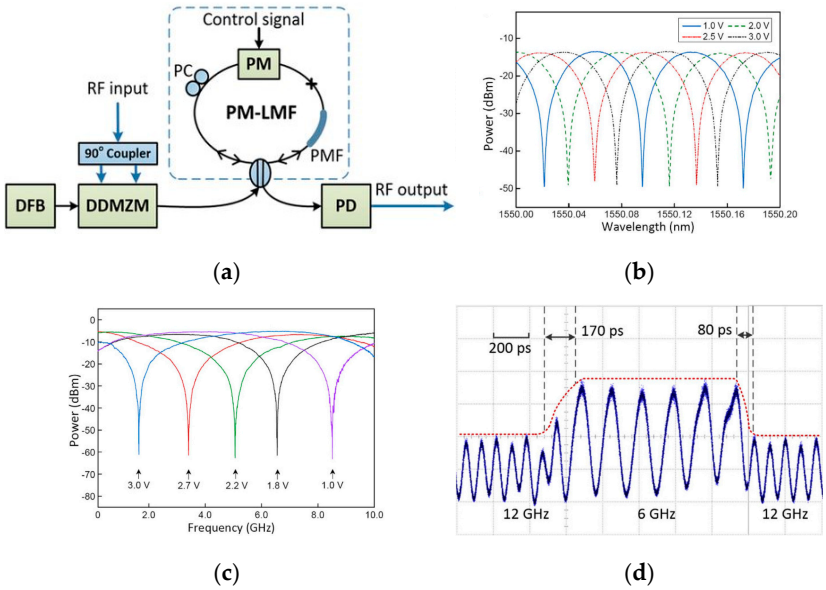

Figure 8. (**a**) Experimental setup of the PM-LMF-based MWP notch filter for RF signal switching. DFB: distributed feedback laser; DD-MZM: dual-drive Mach–Zehnder modulator; PM: phase modulator; PMF: polarization-maintaining fiber; PC: polarization controller; PD: photo detector; (**b**) Measured transmission optical spectra of the tunable PM-LMF at different control voltages. (**c**) Corresponding RF notch filter response at different control voltage; (**d**) Close-up of the frequency-hopping signal that switches between 6 GHz and 12 GHz.

2.4.2. Nonlinear Polarization Rotation Enabled Lyot Loop Filter as an RF Signal Switching

To overcome the periodicity characteristic in the above MWP filter, finite impulse response (FIR)-based MWP bandpass filter can be used instead, such that distinct passbands at the desired frequencies can be obtained. Figure 9a shows the schematic of an optically controlled FIR-based reconfigurable MWP dual-band filter [27]. Unlike the last microwave photonic filter that uses the transmission characteristic of the optical comb to shape the RF frequency response, this MWP dual-band filter uses FIR (i.e., weighting and delaying of RF signal copies for summation) to generate the desired RF filter spectral shape. Moreover, nonlinear polarization rotation in semiconductor optical amplifier (SOA) is used instead as the switching mechanism, where the birefringence in a SOA changes according to the power of a pump light, resulting in polarization rotation of the signal light. A broadband light source is first shaped by an optical Gaussian shape filter and is then spectrally sliced by an optically controlled Lyot loop filter to generate the optical carriers needed for the FIR filter taps. The Lyot loop filter consists of a pair of polarizers (P1, P2), two optical circulators, a length of PMF, a SOA, an OC, and a distributed feedback laser (DFB). As shown in Figure 9b, the circulator-SOA loop enables the input light to transmit through a piece of PMF twice and allow rapid adjustment of the polarization state of the return light through optical injection at the SOA. Within the Lyot loop filter, the input optical signal is linearly polarized at 45° with respect to the principle axis of the PMF. After the first transmission through the PMF, the phase difference $\Delta\varphi$ between fast and slow axis can be expressed as $\Delta\varphi = 2\pi BL/\lambda$, where B and L are the birefringence and length of the PMF, and λ is the light wavelength. Then, the light passes through the circulator-SOA loop and will travel back through the same PMF in the opposite propagation direction with a polarization rotation angle ($\Delta\theta$). By properly modify the optical pump power being injected to the SOA, the polarization rotation angle can be optically switched to 0, 45°, and 90°, resulting in a phase difference switching between $2\Delta\varphi$, $\Delta\varphi$ and 0. Therefore, the resultant phase difference between the light aligned with the two axis changes accordingly to the equivalent length (L_e) of PMF being changed between $2L$, L, and 0. Based on the phase difference, the Lyot loop filter will have the same reconfigurable periodic transmission function as the one described in above section, which is used to spectrally slice the broadband light source. The spectrally sliced optical carrier is then

launched to a dispersive medium to obtain wavelength dependent delay, such that a FIR filter is formed at the photodetector, resulting in a microwave photonic filter with two reconfigurable passbands.

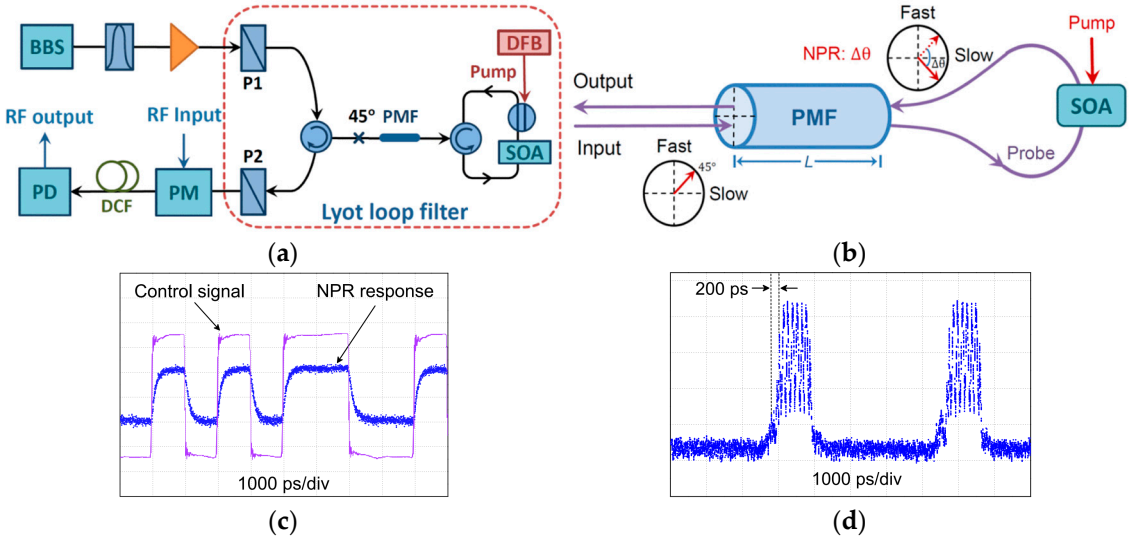

Figure 9. (**a**) Experimental setup of the optically controlled fast reconfigurable microwave photonic dual-band filter for RF signal switching based on nonlinear polarization rotation. BBS: broadband light source. EDFA: erbium-doped fiber amplifier. DFB: distributed feedback laser. SOA: semiconductor optical amplifier. P1–P2: polarizers. PM: phase modulator. PMF: polarization-maintaining fiber. PD: photodetector. DCF: dispersion compensating fiber. (**b**) Operation principle of the optically reconfigurable Lyot loop filter; (**c**) Measured response speed of the nonlinear polarization rotation effect. Purple waveform: 1 Gbps hopping code sequence with a "10101100" pattern. Blue waveform: Corresponding output signal of the SOA that experienced nonlinear polarization rotation. (**d**) Switching speed measurement of the optically controlled RF signal switching with rise/fall time less than 200 ps.

It is important to note that the SOA combined with pump laser works as an optically controllable polarization controller. By applying different optical pump powers, birefringence of the SOA is changed, leading to nonlinear polarization rotation of the light inside the SOA. It has been proven that a polarization rotation angle of up to 180° [49] and a nonlinear polarization rotation response speed at GHz can be achieved [50]. By turning the two reconfigurable passbands in the dual-passband MWP filter on and off via nonlinear polarization rotation in the SOA, either f_1 or f_2 of the input RF signal can be switched out, resulting in a frequency-hopping signal. As a result, ultrafast switching of RF signals via an optically controlled comb filter can be successfully achieved. Figure 9c shows the measurement of nonlinear polarization rotation response speed, where a 1 Gbps "10101100" hopping code sequence is used to modulate the pump laser via an electro-optic intensity modulator. The rise/fall time of the nonlinear polarization rotated output is 200 ps. Figure 9d shows the study of RF signal switching speed and the purity of removing the unwanted frequency. A 6.8 GHz RF signal is used to modulate the optical carrier, and the MWP filter is configured to turn on and off the passband at 6.8 GHz, resulting in an on/off switching of the RF signal with a 200 ps switching speed.

2.5. Integrated Photonic Based MWP Bandpass Filter for Frequency-Hopping Signal Generation

Currently, most photonics-based frequency-hopping systems have been demonstrated using discrete fiber-optic components, which are bulky, with larger loss, and are sensitive to peripheral environment such as temperature changes and vibration, resulting in a significant degradation in the frequency-hopping system performance. Therefore, photonic integration is a necessity to minimize the frequency-hopping system footprint, increase system stability, and make it more comparable with RF circuits [51,52]. Integrated microwave photonics have been used for demonstrating photonic filters [34],

on-chip stimulated Brillouin scattering-based RF signal processor [53], and photonic oscillator based on Kerr comb [54,55]. Regarding the generation of microwave signal on an optical chip, a Kerr optical frequency comb excited in a high-Q magnesium fluoride whispering-gallery-mode resonator was reported to have a phase noise as low as −120 dBc/Hz at a 1-kHz offset frequency [54]. Figure 10 shows the diagram of a fast-switching integrated optical spectral shaper that forms part of an MWP filter (i.e., essentially replacing the Lyot loop filter in the previous section by the optical spectral shaper). The optical spectral shaper chip has a size of 9.6 cm × 2.4 cm, which consists of six delay elements made by silica [34]. The polarization independent 2 × 2 thermal optical switches are used as interconnectors between delay lines, which can be switched between bar-state and cross-state by change the driving voltage. Since six stages of time delay are used in this chip, $2^6 - 1 = 63$ different delay combinations can be obtained. Therefore, the resultant passband frequency can be adjusted through the control of the time delay configuration via the optical switches, as shown in Figure 11a. The fast-switching frequency-hopping signal waveform between 1.782 GHz and 3.635 GHz is shown in Figure 11b, which has a hopping speed of 0.7 ms. So far, the limitation on tuning speed of most integrated photonics circuits and silicon photonic signal processors are governed by the large coefficient of thermal-optic effect [56].

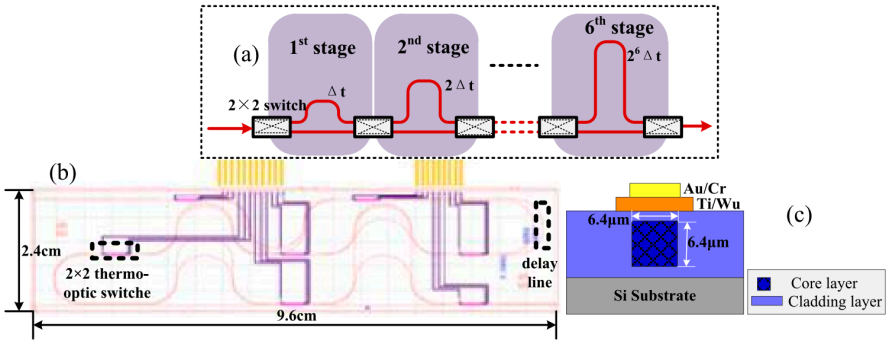

Figure 10. (**a**) Structure diagram of the optical spectral shaper. (**b**) The overall layout of the device. (**c**) Cross-section view of the waveguide (with the courtesy of Dr M. Li).

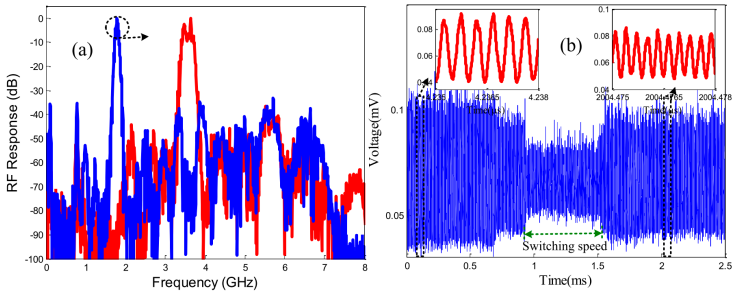

Figure 11. (**a**) Measured frequency response of the single passband microwave photonic filter based on an integrated optical spectral shaper. (**b**) Temporal waveform of the generated frequency-hopping signal, inset: zoom-in view of the two hopping frequencies (with the courtesy of Dr M. Li).

2.6. Real-Time Nonlinear Optical Mixing for Frequency-Hopping Signal Generation

In the above MWP-based frequency-hopping signal-generation schemes, frequency-hopping signal is strongly depending on the center frequencies of the MWP passbands. In this approach, a more flexible allocation of the hopping frequency can be achieved using nonlinear optical mixing for the generation of frequency-hopping signal. Optical nonlinear four wave mixing (FWM) is well known for its transparency to amplitude, phase and frequency [57–59], and has been used for a wide range of signal processing applications, including wavelength conversion, multicasting, parametric amplification, and laser spectroscopy. In this section, the use of FWM for generating frequency-hopping signal with instantaneous hopping speed (Figure 12) will be discussed [23]. The key of the system is to

modulate RF signals on different polarization of the input light—such that only the polarization aligned with that of the hopping code sequence is switched out by FWM. In this approach, a PM is used for polarization modulation by aligning the input optical carrier at 45° with respect to the PM waveguide axes. Therefore, the polarization of the pump light will change with specified hopping code sequence applied onto the PM. In degenerate FWM, FWM efficiency is the strongest if the polarization of the two signals are the same, while no FWM occurs if the polarization of the two signals is orthogonal. Thus, the hopping code sequence modulated pump light will only interact with the either f_1 or f_2 modulated light that has the same polarization.

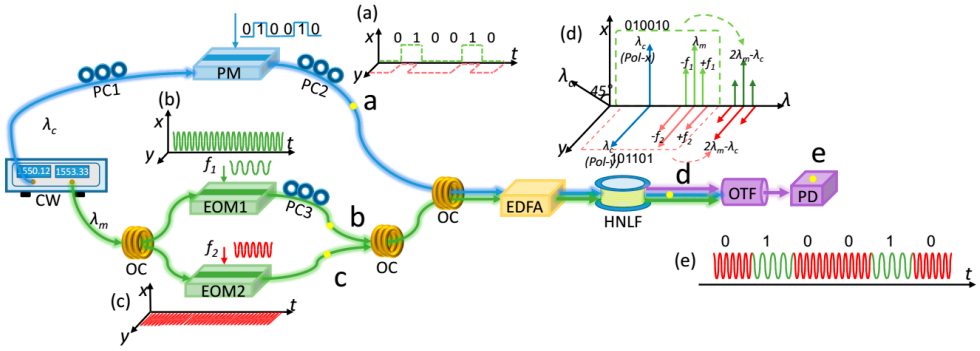

Figure 12. Experimental setup and operation principle of real-time RF switching for frequency hopping system using optical four wave mixing. CW: continuous wavelength laser source; EOM: electro optical modulator; EDFA: Erbium-doped fiber amplifier; HNLF: highly nonlinear fiber; OTF: optical tunable filter; PD: photodetector. (**a**) hopping code sequence; (**b**) and (**c**) modulated RF signals on the same wavelength but different polarization;(**d**) FWM results after HNLF; (**e**) resultant frequency-hopping signals.

In the scheme, the optical carrier at λ_m carries the RF signals f_1 and f_2 at two orthogonal polarizations, while the hopping code sequence for frequency-hopping control is modulated on λ_c, with x polarization to represent bit 1 and y-polarization to represent bit 0. Therefore, only f_1 is switching out when the hopping code sequence is at bit 1, while only f_2 is switched out when the hopping code sequence is at bit 0, as shown in Figure 13a,b. The experiment also shows that switching speed for two-level frequency-hopping signals can be up to tens of picoseconds (<50 ps) resulting from the instantaneous response of nonlinear optical mixing and is currently limited by the rise and fall time of the hopping code sequence, as shown in Figure 13f.

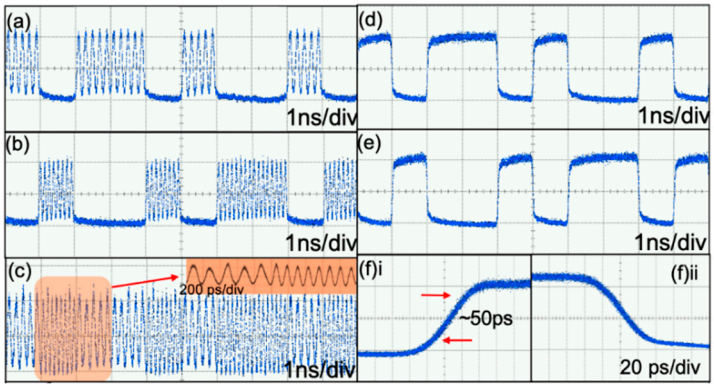

Figure 13. (**a**) and (**b**) Temporal waveforms of only 5 GHz or 8 GHz RF signals when a hopping code sequence of "1011010010" is used in the FWM RF switch; (**c**) Generated frequency-hopping signal between 5 GHz and 8 GHz from FWM RF switch controlled by a "1011010010" code sequence, inset: zoom-in waveform of the orange shaded area; (**d**) and (**e**) FWM outputs at x- and y-polarization when no RF signals are used; (**f**) Response time measurement for (i) Rising and (ii) Falling edge.

3. Adaptive Frequency-Hopping System Bio-Inspired by a Gene of Electric Fish—Eigenmania

The above frequency-hopping systems are solely depending on a hopping code sequence to determine what frequency the system should be using. The applied pseudorandom hopping code sequence (corresponding to channel assignment) is pre-set to achieve a pre-determined frequency-hopping sequence and is only known by the transmitter and target receiver. Frequency-hopping system reduces the possibility of jamming by hopping to different pre-set frequency at different time, resulting in extremely short dwelling time at a particular frequency. To facilitate a dynamic usage of the RF spectrum, it is desirable to have an adaptive frequency-hopping scheme that responses to the population in the RF spectrum, and hops its frequency to the available spot to avoid jamming and increases the use of the whole spectrum effectively. Inspired by the jamming-avoidance response (JAR) in a gene of electric fish—Eigenmania, an adaptive frequency-hopping photonic circuit that is capable of detecting potential jamming and then spectrally moves away from the potential jamming frequency is experimentally demonstrated [60]. By mimicking the JAR neural algorithm with photonics [60–62], the resultant dynamic frequency-hopping system has wideband and instantaneous response benefiting from photonic systems. The dynamic frequency-hopping system is efficient and have adaptive capability thanks to the unique design of the neural algorithm. Figure 14 shows the block diagram of the bio-inspired photonics-based adaptive frequency-hopping system.

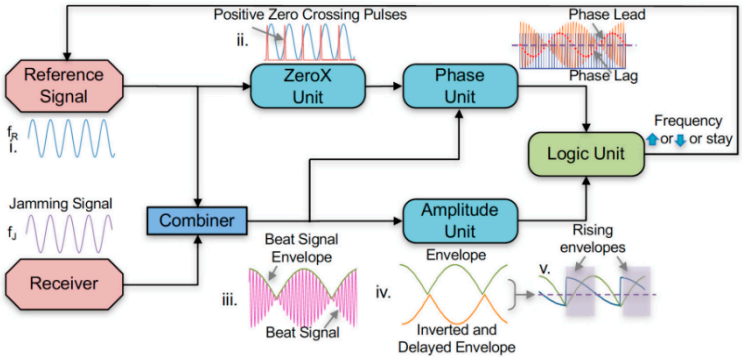

Figure 14. Illustration of the JAR design for adaptive frequency-hopping system. The four functional units are ZeroX unit, Phase unit, Amplitude unit, and Logic unit.

As shown in Figure 14, there are four building blocks that enables the JAR, including (1) Zero-crossing point detection unit (ZeroX unit), (2) Phase detection unit, (3) Amplitude unit, and (4) Logic unit. In the scheme, the reference signal is the current transmitting frequency, while the jamming signal could be the transmitting frequency occupied by another user. All signals are modulated onto optical carriers such that they can be processed in the optical domain using the photonic JAR. The photonic ZeroX unit uses self-phase modulation and offset spectral filtering to generate spikes at the positive zero-crossing points of the reference signal. A beat signal, $S_B(t) = \sin(2\pi f_R t) + \sin(2\pi f_J t)$, between the reference signal and the jamming signal is generated and will be used in the phase unit. The phase unit takes both the zero-crossing spikes and the beat signal as the input, and use cross-gain modulation in SOA to identify the phase relationship between them. The beat signal is the pump that tries to deplete the carriers in the SOA to induce cross-gain modulation, while the zero-crossing point spikes are the probe signal that could experience the cross-gain modulation effect. Each peak in the beat signal and the zero-crossing spikes are a pair, which is either able or not able to have cross-gain modulation, depending on the phase relationship within the pair. If the phase of the beat signal is leading, the peak of the beat signal enters the SOA before the zero-crossing spike and causes cross-gain modulation to the zero-crossing spike. On the other hand, if the phase of the beat signal is lagging, the peak of the beat signal enters the SOA after the zero-crossing spike, making it unable to cause cross-gain modulation to the zero-crossing spike. Therefore, a weak zero-crossing spike is resulted if

the phase of the beat signal is leading, while a strong zero-crossing spike is resulted if the phase of the beat signal is lagging. Then, the amplitude unit takes the envelope of the beat signal and make an inverted copy using cross-gain modulation at an SOA. By adding the non-inverted beat signal envelope with a delayed inverted beat signal envelope, a high output is resulted if the envelope amplitude is increasing, while a low output is resulted if the envelope amplitude is decreasing. Lastly, the logic unit takes the phase and amplitude information and determine if the JAR should increase, decrease, or maintain the reference signal frequency based on a XOR relationship.

Figure 15 shows the spectral waterfall of the reference signal measured by a software-defined radio (SDR) that represents how the reference signal adaptively hops to a different frequency when a jammer is approaching it spectrally. Figure 15a,b corresponds to a lower jamming frequency (in the red box), while Figure 15c,d corresponds to a higher jamming frequency (in the red box). The JAR maintains a minimum frequency separation of 150 MHz between the jammer and the reference signal by hopping to a different frequency when it is spectrally too close.

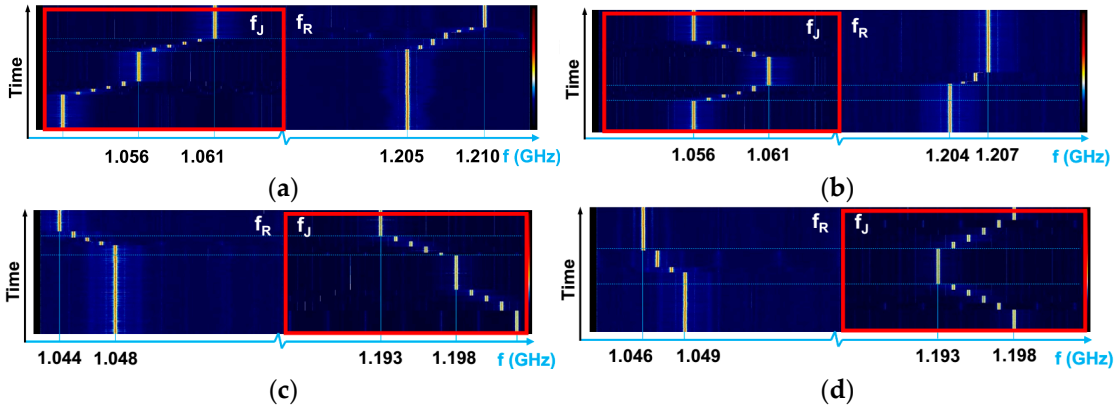

Figure 15. Spectral waterfall measurement of the photonic JAR in action with sinusoidal reference signal f_R and jamming signals f_J.(**a**) The jamming signal f_J is approaching f_R from the low frequency side and triggers the JAR, (**b**) The jamming signal f_J is approaching f_R from the low frequency side and triggers the JAR, and then is moved away, (**c**) The jamming signal f_J is approaching f_R from the high-frequency side and triggers the JAR, (**d**) The jamming signal f_J is approaching f_R from the high-frequency side and triggers the JAR and then is moved away.

4. Discussions and Conclusions

This paper reviews several state-of-the-art microwave photonic frequency-hopping systems that enable fast frequency-hopping for wireless RF systems. Frequency-hopping systems has the potential to improve information security, mitigate jamming and interference, and increase spectral efficiency, which are of great interest in military, commercial, and consumer applications. Microwave photonics have been promising in providing improved hopping speed and frequency-hopping bandwidth compared to its electronic counterparts, which essentially increases the capability of data transmission, improves information security as well as enhanced signal fidelity. Recent advancement in microwave photonic frequency-hopping schemes enable hopping speed ranging from picoseconds to nanoseconds and the hopping-frequency bandwidth over tens of GHz with hopping stability. Moreover, some of the microwave photonic approaches could be used for multi-level frequency-hopping, including flexible OEOs, tunable MWP filters, and nonlinear period-one dynamics in lasers. To achieve both multi-level frequency-hopping and fast switching speed, multiple frequency-hopping approaches with fast switching time could be incorporated together to increase the level of frequency-hopping while maintaining the high hopping speed.

The rapid development of real-time frequency-hopping speed as well as the transparency of data formats, frequency, phase and amplitude in the frequency-hopping system could be potentially used in the future THz wireless communication and be used in any wireless communication

transmission scenario. Furthermore, the development of bio-inspired adaptive frequency-hopping system could identify the available hopping frequency and simultaneously allow the jamming-free frequency-hopping data transmission. Looking forward, the practical application of microwave photonic frequency-hopping system can be further improved and optimized by miniature, integration, and incorporating intelligence to adapt to more sophisticated wireless communications.

Author Contributions: Resources and Review, Q.L.; Project Administration and Supervision, M.P.F.; All authors contributed to data analysis and manuscript writing. All authors have read and agreed to the published version of the manuscript.

Funding: The research work is supported by research grant from National Science Foundation, grant numbers ECCS 1653525 and ECCS 1917043.

Conflicts of Interest: The authors declare no conflict of interest.

References

1. Simon, M.K.; Omura, J.K.; Scholtz, R.A.; Levitt, B.K. *Spread Spectrum Communications Handbook*; McGraw-Hill: New York, NY, USA, 1994; Volume 2.
2. Hu, W.; Willkomm, D.; Abusubaih, M.; Gross, J.; Vlantis, G.; Gerla, M.; Wolisz, A. Dynamic frequency hopping communities for efficient IEEE 802.22 operation. *IEEE Commun. Mag.* **2007**, *45*, 80–87. [CrossRef]
3. Mahafza, B.R. *Introduction to Radar Analysis*; Chapman and Hall/CRC: Boca Raton, FL, USA, 2017.
4. Aykin, I.; Krunz, M.; Xiao, Y. Adaptive frequency-hopping schemes for CR-based multi-link satellite networks. *Int. J. Satell. Commun. Netw.* **2018**, *36*, 315–331. [CrossRef]
5. Muller, N.J. *Bluetooth Demystified*; McGraw-Hill: New York, NY, USA, 2001; Volume 1.
6. Fritz, D.A.; Moy, D.W.; Nichols, R.A. Modeling and simulation of Advanced EHF efficiency enhancements. In Proceedings of the MILCOM, Atlantic City, NJ, USA, 31 October–3 November 1999; pp. 354–358.
7. Montgomery, J.; Runyon, D.; Fuller, J. Large multibeam lens antennas for EHF SATCOM. In Proceedings of the MILCOM 88, 21st Century Military Communications-What's Possible? Conference record, Military Communications Conference, San Diego, CA, USA, 23–26 October 1988; pp. 369–373.
8. Capmany, J.; Novak, D. Microwave photonics combines two worlds. *Nat. Photonics* **2007**, *1*, 319. [CrossRef]
9. Liu, Q.; Yan, J.; Xin, F. Microwave waveform generation with reconfigurable envelope and high fidelity based on spectrum compensated frequency-to-time mapping. *Opt. Fiber Technol.* **2017**, *36*, 291–296. [CrossRef]
10. Pan, S.; Zhang, Y. Tunable and wideband microwave photonic phase shifter based on a single-sideband polarization modulator and a polarizer. *Opt. Lett.* **2012**, *37*, 4483–4485. [CrossRef]
11. Fok, M.; Lee, K.; Shu, C. 4/spl times/2.5 GHz repetitive photonic sampler for high-speed analog-to-digital signal conversion. *IEEE Photonics Technol. Lett.* **2004**, *16*, 876–878. [CrossRef]
12. Liu, Q.; Fok, M.P. Dual-Function Frequency and Doppler Shift Measurement System using a Phase Modulator Incorporated Lyot Filter. In Proceedings of the Optical Fiber Communications Conference and Exhibition, San Diego, CA, USA, 3–7 March 2019; pp. 1–3.
13. Xin, F.; Yan, J.; Liu, Q. Microwave frequency measurement based on optical phase modulation and stimulated Brillouin scattering. *Electron. Lett.* **2017**, *53*, 937–939. [CrossRef]
14. Su, F.; Wu, G.; Chen, J. Photonic analog-to-digital conversion with equivalent analog prefiltering by shaping sampling pulses. *Opt. Lett.* **2016**, *41*, 2779–2782. [CrossRef] [PubMed]
15. Ma, Y.; Liang, D.; Peng, D.; Zhang, Z.; Zhang, Y.; Zhang, S.; Liu, Y. Broadband high-resolution microwave frequency measurement based on low-speed photonic analog-to-digital converters. *Opt. Express* **2017**, *25*, 2355–2368. [CrossRef] [PubMed]
16. Dai, Y.; Li, J.; Zhang, Z.; Yin, F.; Li, W.; Xu, K. Real-time frequency-to-time mapping based on spectrally-discrete chromatic dispersion. *Opt. Express* **2017**, *25*, 16660–16671. [CrossRef] [PubMed]
17. Yao, J. Photonics to the rescue: A fresh look at microwave photonic filters. *IEEE Microw. Mag.* **2015**, *16*, 46–60. [CrossRef]
18. Zhang, J.; Chan, E.H.W.; Wang, X.; Feng, X.; Guan, B. High conversion efficiency photonic microwave mixer with image rejection capability. *IEEE Photonics J.* **2016**, *8*, 1–11. [CrossRef]
19. Zhu, D.; Hu, X.; Chen, W.; Ben, D.; Pan, S. Photonics-enabled simultaneous self-interference cancellation and image-reject mixing. *Opt. Lett.* **2019**, *44*, 5541–5544. [CrossRef] [PubMed]

20. Azaña, J.; Chen, L.R. Synthesis of temporal optical waveforms by fiber Bragg gratings: A new approach based on space-to-frequency-to-time mapping. *J. Opt. Soc. Am. B* **2002**, *19*, 2758–2769. [CrossRef]
21. Tseng, C.-H.; Hung, Y.-H.; Hwang, S.-K. Frequency-modulated continuous-wave microwave generation using stabilized period-one nonlinear dynamics of semiconductor lasers. *Opt. Lett.* **2019**, *44*, 3334–3337. [CrossRef] [PubMed]
22. Zhou, P.; Li, N.; Pan, S. Photonic microwave harmonic down-converter based on stabilized period-one nonlinear dynamics of semiconductor lasers. *Opt. Lett.* **2019**, *44*, 4869–4872. [CrossRef]
23. Liu, Q.; Fok, M.P. Real-time Temporal Signal Stitching Using Polarization-Dependent Optical Wave Mixing. In Proceedings of the Frontiers in Optics, Washington, DC, USA, 15–19 September 2019; p. FTu5B. 4.
24. Jiang, H.; Yan, L.; Pan, W.; Luo, B.; Zou, X. Ultra-high speed RF filtering switch based on stimulated Brillouin scattering. *Opt. Lett.* **2018**, *43*, 279–282. [CrossRef]
25. Jiang, H.; Yan, L.; Pan, Y.; Pan, W.; Luo, B.; Zou, X.; Eggleton, B. Microwave photonic comb filter with ultra-fast tunability. *Opt. Lett.* **2015**, *40*, 4895–4898. [CrossRef]
26. Ge, J.; Fok, M.P. Ultra high-speed radio frequency switch based on photonics. *Sci. Rep.* **2015**, *5*, 17263. [CrossRef]
27. Ge, J.; Fok, M.P. Optically controlled fast reconfigurable microwave photonic dual-band filter based on nonlinear polarization rotation. *IEEE Trans. Microw. Theory Tech.* **2016**, *65*, 253–259. [CrossRef]
28. Chen, Y. High-speed and wideband frequency-hopping microwave signal generation via switching the bias point of an optical modulator. *IEEE Photonics J.* **2018**, *10*, 1–7. [CrossRef]
29. Zhou, P.; Zhang, F.; Ye, X.; Guo, Q.; Pan, S. Flexible frequency-hopping microwave generation by dynamic control of optically injected semiconductor laser. *IEEE Photonics J.* **2016**, *8*, 1–9. [CrossRef]
30. Supradeepa, V.; Long, C.M.; Wu, R.; Ferdous, F.; Hamidi, E.; Leaird, D.E.; Weiner, A.M. Comb-based radio-frequency photonic filters: Routes to nanosecond tuning speed and extremely high stopband attenuation. *arXiv* **2011**, arXiv:1105.0722.
31. Li, W.; Zhang, W.; Yao, J. Frequency-hopping microwave waveform generation based on a frequency-tunable optoelectronic oscillator. In Proceedings of the Optical Fiber Communication Conference, San Francisco, CA, USA, 9–13 March 2014; pp. 1–3.
32. Zhou, F.; Wang, X.; Yan, S.; Hu, X.; Zhang, Y.; Qiu, H.; Xiao, X.; Dong, J.; Zhang, X. Frequency-hopping microwave generation with a large time-bandwidth product. *IEEE Photonics J.* **2018**, *10*, 1–9. [CrossRef]
33. Hindle, P. The state of RF/microwave switches. *Microw. J.* **2010**, *53*, 20–36.
34. Shi, N.; Zhu, X.; Sun, S.; Li, W.; Zhu, N.; Li, M. Fast-Switching Microwave Photonic Filter Using an Integrated Spectrum Shaper. *IEEE Photonics Technol. Lett.* **2019**, *31*, 269–272. [CrossRef]
35. Yan, J.; Liang, A.; Xin, F.; Liu, Q. An Optical Microwave Generator based on Stimulated Brillouin Scattering with Fine Tunability. In Proceedings of the Conference on Lasers and Electro-Optics, San Jose, CA, USA, 13–18 May 2018; pp. 1–2.
36. Cheng, Y.; Yan, J.; Zhao, S. Self-Oscillating Parametric Optical Frequency Comb Generation Using an Electroabsorption Modulated Laser-Based Optoelectronic Oscillator. *IEEE Photonics J.* **2019**, *11*, 1–9. [CrossRef]
37. Liu, A.; Dai, J.; Xu, K. Stable and Low-Spurs Optoelectronic Oscillators: A Review. *Appl. Sci.* **2018**, *8*, 2623. [CrossRef]
38. Hunter, I.; Rhodes, J.D. Electronically tunable microwave bandpass filters. *IEEE Trans. Microw. Theory Tech.* **1982**, *30*, 1354–1360. [CrossRef]
39. Zhang, X.Y.; Xue, Q.; Chan, C.H.; Hu, B.-J. Low-loss frequency-agile bandpass filters with controllable bandwidth and suppressed second harmonic. *IEEE Trans. Microw. Theory Tech.* **2010**, *58*, 1557–1564. [CrossRef]
40. Zhang, L.; Chan, S.-C. Cascaded injection of semiconductor lasers in period-one oscillations for millimeter-wave generation. *Opt. Lett.* **2019**, *44*, 4905–4908. [CrossRef]
41. Usechak, N.G.; Suelzer, J.S.; Haefner, J.W. High-speed wideband voltage-controlled oscillator via an injection-locked laser. *IEEE Photonics Technol. Lett.* **2017**, *29*, 1132–1135. [CrossRef]
42. Ge, J.; Garon, D.A.; Liu, Q.; Fok, M.P. Reconfigurable microwave photonic spectral shaper. In Proceedings of the Optical Fiber Communication Conference, San Diego, CA, USA, 3–7 March 2019; pp. 1–3.
43. Ge, J.; Fok, M.P. Passband switchable microwave photonic multiband filter. *Sci. Rep.* **2015**, *5*, 15882. [CrossRef]

44. Fok, M.P.; Ge, J.; Liu, Q. Dynamic and multiband RF spectral processing. In Proceedings of the Smart Photonic and Optoelectronic Integrated Circuits XXI, San Francisco, CA, USA, 4 March 2019; pp. 105–113.
45. Marpaung, D.; Morrison, B.; Pagani, M.; Pant, R.; Choi, D.-Y.; Luther-Davies, B.; Madden, S.J.; Eggleton, B.J. Low-power, chip-based stimulated Brillouin scattering microwave photonic filter with ultrahigh selectivity. *Optica* **2015**, *2*, 76–83. [CrossRef]
46. Liu, Q.; Ge, J.; Fok, M.P. Microwave photonic multiband filter with independently tunable passband spectral properties. *Opt. Lett.* **2018**, *43*, 5685–5688. [CrossRef]
47. Hamidi, E.; Leaird, D.E.; Weiner, A.M. Tunable programmable microwave photonic filters based on an optical frequency comb. *IEEE Trans. Microw. Theory Tech.* **2010**, *58*, 3269–3278. [CrossRef]
48. Ge, J.; Feng, H.; Scott, G.; Fok, M.P. High-speed tunable microwave photonic notch filter based on phase modulator incorporated Lyot filter. *Opt. Lett.* **2015**, *40*, 48–51. [CrossRef]
49. Fu, S.; Wang, M.; Zhong, W.-D.; Shum, P.; Wen, Y.J.; Wu, J.; Lin, J. SOA nonlinear polarization rotation with linear polarization maintenance: Characterization and applications. *IEEE J. Sel. Top. Quantum Electron.* **2008**, *14*, 816–825. [CrossRef]
50. Mathlouthi, W.; Vacondio, F.; Lemieux, P.; Rusch, L.A. SOA gain recovery wavelength dependence: Simulation and measurement using a single-color pump-probe technique. *Opt. Express* **2008**, *16*, 20656–20665. [CrossRef]
51. Marpaung, D.; Roeloffzen, C.; Heideman, R.; Leinse, A.; Sales, S.; Capmany, J. Integrated microwave photonics. *Laser Photonics Rev.* **2013**, *7*, 506–538. [CrossRef]
52. Zou, X.; Zou, F.; Cao, Z.; Lu, B.; Yan, X.; Yu, G.; Deng, X.; Luo, B.; Yan, L.; Pan, W. A Multifunctional Photonic Integrated Circuit for Diverse Microwave Signal Generation, Transmission, and Processing. *Laser Photonics Rev.* **2019**, *13*, 1800240. [CrossRef]
53. Marpaung, D.; Pagani, M.; Morrison, B.; Eggleton, B.J. Nonlinear integrated microwave photonics. *J. Light. Technol.* **2014**, *32*, 3421–3427. [CrossRef]
54. Liang, W.; Eliyahu, D.; Ilchenko, V.S.; Savchenkov, A.A.; Matsko, A.B.; Seidel, D.; Maleki, L. High spectral purity Kerr frequency comb radio frequency photonic oscillator. *Nat. Commun.* **2015**, *6*, 7957. [CrossRef] [PubMed]
55. Xue, X.; Xuan, Y.; Liu, Y.; Wang, P.-H.; Chen, S.; Wang, J.; Leaird, D.E.; Qi, M.; Weiner, A.M. Mode-locked dark pulse Kerr combs in normal-dispersion microresonators. *Nat. Photonics* **2015**, *9*, 594. [CrossRef]
56. Reed, G.T.; Mashanovich, G.; Gardes, F.Y.; Thomson, D. Silicon optical modulators. *Nat. Photonics* **2010**, *4*, 518. [CrossRef]
57. Fok, M.P.; Prucnal, P.R. Polarization Effect on OpticalxorPerformance Based on Four-Wave Mixing. *IEEE Photonics Technol. Lett.* **2010**, *22*, 1096–1098. [CrossRef]
58. Fok, M.P.; Prucnal, P.R. All-optical XOR gate with optical feedback using highly Ge-doped nonlinear fiber and a terahertz optical asymmetric demultiplexer. *Appl. Opt.* **2011**, *50*, 237–241. [CrossRef]
59. Yu, C.; Christen, L.; Luo, T.; Wang, Y.; Pan, Z.; Yan, L.-S.; Willner, A.E. All-optical XOR gate using polarization rotation in single highly nonlinear fiber. *IEEE Photonics Technol. Lett.* **2005**, *17*, 1232–1234.
60. Lin, R.; Ge, J.; Tran, P.; Perea, L.A.; Toole, R.; Fok, M.P. Biomimetic photonics: Jamming avoidance system in Eigenmannia. *Opt. Express* **2018**, *26*, 13349–13360. [CrossRef]
61. Toole, R.; Fok, M.P. A photonic RF jamming avoidance response system bio-inspired by Eigenmannia. In Proceedings of the Optical Fiber Communications Conference and Exhibition (OFC), Anaheim, CA, USA, 20–24 March 2016; pp. 1–3.
62. Toole, R.; Fok, M.P. Photonic implementation of a neuronal algorithm applicable towards angle of arrival detection and localization. *Opt. Express* **2015**, *23*, 16133–16141. [CrossRef]